

Electrostatic Steering and Ionic Tethering in the Formation of Thrombin–Hirudin Complexes: The Role of the Thrombin Anion-Binding Exosite-I[†]

Timothy Myles,* Bernard F. Le Bonniec,[‡] Andreas Betz,[§] and Stuart R. Stone^{||}

Department of Haematology, University of Cambridge, MRC Centre, Hills Road, Cambridge CB2 2QH, United Kingdom, and
Department of Biochemistry and Molecular Biology, Monash University, Clayton, Victoria 3168, Australia

Received October 9, 2000; Revised Manuscript Received January 9, 2001

ABSTRACT: Electrostatic interactions between the thrombin anion-binding exosite-I (ABE-I) and the hirudin C-terminal tail play an important role in the formation of the thrombin–hirudin inhibitor complex and serves as a model for the interactions of thrombin with its many other ligands. The role of each solvent exposed basic residue in ABE-I (Arg³⁵, Lys³⁶, Arg⁶⁷, Arg⁷³, Arg⁷⁵, Arg^{77a}, Lys⁸¹, Lys¹⁰⁹, Lys¹¹⁰, and Lys^{149e}) in electrostatic steering and ionic tethering in the formation of thrombin–hirudin inhibitor complexes was explored by site directed mutagenesis. The contribution to the binding energy (ΔG_b^o) by each residue varied from 1.9 kJ mol⁻¹ (Lys¹¹⁰) to 15.3 kJ mol⁻¹ (Arg⁷³) and were in general agreement to their observed interactions with hirudin residues in the thrombin–hirudin crystal structure [Rydel, T. J., Tulinsky, A., Bode, W., and Huber, R. (1991) *J. Mol. Biol.* 221, 583–601]. Coupling energies ($\Delta\Delta G_{int}^o$) were calculated for the major ion-pair interactions involved in ionic tethering using complementary hirudin mutants (h-D55N, h-E57Q, and h-E58Q). Cooperativity was seen for the h-Asp⁵⁵/Arg⁷³ ion pair ($\Delta\Delta G_{int}^o$ 2.4 kJ mol⁻¹); however, low coupling energies for h-Asp⁵⁵/Lys^{149e} ($\Delta\Delta G_{int}^o$ 0.6 kJ mol⁻¹) and h-Glu⁵⁸/Arg^{77a} ($\Delta\Delta G_{int}^o$ 0.9 kJ mol⁻¹) suggest these are not major interactions, as anticipated by the crystal structure. Interestingly, high coupling energies were seen for the intermolecular ion-pair h-Glu⁵⁷/Arg⁷⁵ ($\Delta\Delta G_{int}^o$ 2.3 kJ mol⁻¹) and for the solvent bridge h-Glu⁵⁷/Arg^{77a} ($\Delta\Delta G_{int}^o$ 2.7 kJ mol⁻¹) indicating that h-Glu⁵⁷ interacts directly with both Arg⁷⁵ and Arg^{77a} in the thrombin–hirudin inhibitor complex. The remaining ABE-I residues that do not form major contacts in tethering the C-terminal tail of hirudin make small but collectively important contributions to the overall positive electrostatic field generated by ABE-I important in electrostatic steering.

Human thrombin is a trypsin-like serine protease characterized by two anion-binding exosites adjacent to the active site which are necessary for the binding of several ligands to overcome steric hindrance of the occluded active site cleft (1). Anion-binding exosite-I (ABE-I)¹ has been shown to be important for the binding of fibrinogen (2–5), fibrin (6), HCII (7, 8), PAR1 (9, 10), thrombomodulin (5, 11–13), and the leech inhibitor hirudin (14–17). Anion-binding exosite-II (ABE-II) is principally involved in the binding of glycosaminoglycan bound serpins ATIII (7, 18, 19), HCII (7, 8, 18), and PN1 (20, 21). Both exosites have been implicated in the binding of the coagulation factors V and VIII (22). Kinetic studies on the inhibition of thrombin with recombinant hirudin (rhir) have shown that electrostatic interactions between ABE-I and the C-terminal tail of hirudin

are important for the rate of complex formation and the stability of the complex (23) and as such, are likely to be applicable for all the ligands that bind to ABE-I. The crystal structure of human thrombin complexed with recombinant hirudin [variant 1] (15–17) reveals the globular N-terminal domain of hirudin lying over the active site cleft of thrombin. The C-terminal tail, rich with acidic amino acids, extends away from the active site toward the ABE-I where it participates in several electrostatic, hydrogen bonding and hydrophobic contacts. The major electrostatic interactions between the C-terminal tail of hirudin and the ABE-I are ion-pair interactions between h-Glu⁴⁹ (the h-preceding the amino acid denotes a hirudin residue) and Lys^{60f},² h-Asp⁵⁵ with both Arg⁷³ and Lys^{149e}, h-Glu⁵⁸ and Arg^{77a}, and the C-terminal h-Gln⁶⁵ carboxylate and Lys³⁶. An intermolecular ion-pair interaction is also seen between h-Glu⁵⁷ and Arg⁷⁵ from a neighboring thrombin molecule occurs in the crystal lattice (17). Site directed mutagenesis studies have indicated that each negatively charged hirudin C-tail residue (h-Asp⁵⁵, h-Glu⁵⁷, h-Glu⁵⁸, h-Glu⁶¹, and h-Glu⁶²) contributes to the binding energy for the stabilization of the thrombin–hirudin complex including h-Glu⁶¹ and h-Glu⁶², despite the fact the side chains of these residues are pointing into the solvent

[†] This research was supported by the British Heart Foundation of Great Britain.

* To whom correspondence should be addressed. Phone: +1 (650) 725 4043. Fax: +1 (650) 736 0974. E-mail: tmyles@stanford.edu.

[‡] INSERM U428, Université Paris V, 4 avenue de l'Observatoire, 75270 Paris Cedex 06, France.

[§] Cor Therapeutics, Inc., 256 E. Grand Ave., South San Francisco, CA 94080.

^{||} This paper is dedicated to the memory of Prof. Stuart R. Stone at Monash University.

¹ Abbreviations: ABE, anion binding exosite; PAR1, protease activated receptor 1; HCII, Heparin cofactor II; ATIII, antithrombin III; PN1, protease nexin 1; pNA, p-nitroaniline; rhir, recombinant hirudin.

² The numbering of thrombin residues is based on chymotrypsinogen numbering. Insertions are shown as superscripted letters in alphabetical order [e.g., Lys^{149e} is the 5th (e) residue inserted at position 149].

and make no ionic contacts (24). Theoretical calculation of electrostatic fields surrounding the thrombin ABE-I and the hirudin acidic C-terminal tail show the residues h-Glu⁶¹ and h-Glu⁶² could contribute to the electrostatic field (25). These electrostatic fields are asymmetric and complementary and protrude into the solvent where they preorientate and increase the rate of complex formation by the process of "electrostatic steering" (25). In general, theoretical calculations agree with site directed mutagenesis studies showing a significant contribution of binding energy by hirudin residues for the generation of an electrostatic field including the residues h-Glu⁶¹ and h-Glu⁶² (24).

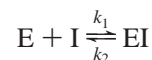
To fully understand the contribution of ABE-I basic residues for "electrostatic steering" (25) and the formation of direct ion-pairs in "ionic tethering" (26) for complex formation, we determined the contribution made by the basic residues in ABE-I (Arg³⁵, Lys³⁶, Arg⁶⁷, Arg⁷³, Arg⁷⁵, Arg^{77a}, Lys⁸¹, Lys¹⁰⁹, Lys¹¹⁰, and Lys^{149e}) to the binding energy for the formation of the thrombin–hirudin complex. Double mutant cycles were constructed with complementary hirudin mutants to assess how ion-pair interactions contribute to the binding of the hirudin C-terminal tail to ABE-I and how cooperative the interactions are over the interaction interface. Surprisingly, the double mutant cycles were particularly useful in probing ambiguities between the thrombin–hirudin crystal structure and kinetic studies for the formation of the thrombin–hirudin inhibitor complex. Defining the contribution of basic residues in ABE-I for complex formation is beneficial in understanding how thrombin delineates its specificity toward its many substrates, receptors, and inhibitors through electrostatic steering and ionic tethering, which would lead to the coherent design of antithrombotic agents.

EXPERIMENTAL SECTION

Materials. The chromogenic substrate H-D-Phe-Pip-Arg-*p*-nitroanilide (S-2238) was purchased from Chromogenix (Quadrant, Surrey, U.K.). Human plasma thrombin was purified to homogeneity from slow bleed plasmas described previously (27) and active site titrated with *p*-nitrophenol *p*'-guanidinobenzene to determine the concentration of active thrombin molecules (28). The expression, purification and determination of the concentrations of recombinant native (rhir) and the variant hirudins h-D55N,³ h-E57Q, h-E58Q, h-E57Q–E58Q (h-E57–58Q), and h-E57Q–E58Q–E61Q–E62Q (h-E57–58–61–62Q) have been described previously (25, 29). Human recombinant native and mutant thrombins was prepared from insect cells using the baculovirus system as described previously (8).

Kinetic Assays and Data Analysis. All amidolytic thrombin assays were performed at 37 °C in 50 mM Tris-HCl, pH 8.0, 100 mM NaCl, 0.1% w/v poly(ethylene glycol) (*M*_r 6000) as described previously (27). Values for *K*_m and *k*_{cat} for the hydrolysis of the substrate H-D-Phe-Pip-Arg-*p*NA (S2238) by wild-type and mutant recombinant thrombins were determined by measuring the initial rates of hydrolysis of H-D-Phe-Pip-Arg-*p*NA over a range of H-D-Phe-Pip-Arg-

*p*NA concentrations. The initial reaction velocities were plotted against [S] and then fitted to the Michaelis–Menten equation by nonlinear regression analysis to determine the values of *K*_m and *k*_{cat}. Hirudin is a slow tight-binding inhibitor of thrombin (27) and the minimum kinetic mechanism which describes the interaction of hirudin (I) with thrombin (E) is given by the following scheme:



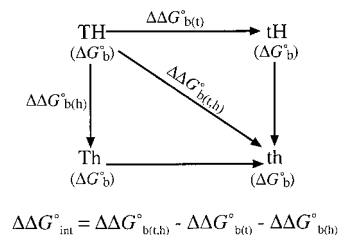
The dissociation constant for the complex (*K*₁) can be related the overall association rate constant (*k*₁) and the overall dissociation rate constant (*k*₂) by the expression *K*₁ = *k*₂/*k*₁. For the majority of native and mutant thrombins and hirudins, estimates of *K*₁, *k*₁, and *k*₂ were obtained by analyzing progress curves for the thrombin catalyzed formation of *p*-nitroaniline from the substrate H-D-Phe-Pip-Arg-*p*NA in the presence of different concentrations of hirudin. Each progress curve was analyzed according to the equation for slow tight-binding inhibition (30) and the estimates for the apparent dissociation constant (*K*₁') and apparent association rate constant (*k*₁') were calculated as described previously (14). The true values for *K*₁ and *k*₁ were adjusted by correcting for the concentration of substrate (29). When non linear competitive inhibition was observed, the values for the inhibition constants *K*₁₁ and *K*₁₂ were calculated for two forms of mutant thrombin (31).

The Gibbs standard free energy change for the formation of the thrombin–hirudin complex (denoted as the binding energy, Δ*G*_b^o) can be calculated from the value of *K*₁ using the following relationship:

$$\Delta G_b^o = RT \ln K_1$$

where *T* is the absolute temperature of the assay (in Kelvin) and *R* is the universal gas constant.

Analysis of Cooperative Interactions Using Double Mutant Cycles. Double mutant cycles were constructed to measure intermolecular pairwise interactions between basic residues in the thrombin ABE-I and acidic residues in the hirudin C-terminal tail by determining the coupling energy (ΔΔ*G*_{int}^o) as follows (32, 33):



ΔΔ*G*_{b(t,h)}^o reflects the difference in the Δ*G*_b^o between the double mutant (t,h) and the wild-type (T,H) while ΔΔ*G*_{b(t)}^o and ΔΔ*G*_{b(h)}^o are the differences between the mutants t and h and wild-type T and H, respectively. The value for ΔΔ*G*_{int}^o indicates the extent to which a mutation at one residue affects the contribution of the other residue to the binding energy. When ΔΔ*G*_{int}^o = 0, the pair of residues analyzed do not interact, i.e., the effect of the two mutations are additive. When there is cooperativity between two sites, ΔΔ*G*_{int}^o ≠ 0, then the mutational effects are nonadditive.

³ Standard nomenclature is used to describe mutant thrombins and hirudins. The first letter shows the amino acid in the wild-type to be replaced, and the second letter shows the amino acid used for the substitution (e.g., the mutant thrombin K149Q represents the substitution of Lys^{149e} with Gln).

Table 1: Kinetic Parameters for the Cleavage of H-D-Phe-Pip-Arg-pNA by Wild-Type and Mutant Thrombins^a

thrombin	K_m (μM)	k_{cat} (s^{-1})	k_{cat}/K_m ($\text{M}^{-1} \text{s}^{-1} \times 10^{-7}$)
rIIa	3.6 ± 0.2	215.6 ± 4.1	5.99
pIIa	4.4 ± 0.6	236.0 ± 10.4	5.36
R35Q	3.7 ± 0.4	187.9 ± 5.2	5.08
K36Q	3.6 ± 0.5	175.0 ± 9.9	4.86
R67Q	4.5 ± 0.5	266.3 ± 10.5	5.92
R73Q	5.6 ± 0.5	284.3 ± 8.9	5.08
R75Q	3.5 ± 0.4	185.7 ± 0.4	6.08
R77 ^a Q	4.1 ± 0.4	228.3 ± 7.0	5.57
K81Q	4.5 ± 0.2	224.5 ± 3.8	4.99
K109Q	3.4 ± 0.4	185.7 ± 4.5	5.44
K110Q	3.4 ± 0.4	237.7 ± 8.1	6.99
K149 ^a Q	3.0 ± 0.1	187.0 ± 14.8	6.23

^a Assays to determine the values for K_m and k_{cat} were performed as described in the experimental procedures section. The concentration of thrombin was 20 pM and the concentration of H-D-Phe-Pip-Arg-pNA was varied from 2 to 20 μM (six data points). The initial velocities were fitted to the Michaelis–Menten equation using weighted linear regression (11). These analyses gave the values for the kinetic constants and are given in the table together with their standard errors.

When $\Delta\Delta G_{\text{int}}^{\circ}$ is positive the residues interact favorably while a negative value for $\Delta\Delta G_{\text{int}}^{\circ}$ indicates the two residues interact unfavorably.

RESULTS

Cleavage of H-D-Phe-Pip-Arg-pNA Chromogenic Substrate. The catalytic activity of thrombin to the chromogenic substrate H-D-Phe-Pip-Arg-pNA was investigated using Michaelis–Menten kinetics. The values for K_m and k_{cat} for the hydrolysis of H-D-Phe-Pip-Arg-pNA by plasma and recombinant thrombin are 4.4 μM and 236 s^{-1} and 3.6 μM and 216 s^{-1} , respectively. There were no significant differences between K_m , k_{cat} and the specificity constant (k_{cat}/K_m) for the hydrolysis of chromogenic substrate by the variant thrombins when compared to plasma and recombinant wild-type thrombin (Table 1).

Inhibition of Thrombin Mutants by rhir. Values for the association rate constant (k_{on}) and the inhibition constant (K_i) were determined for the inhibition of plasma and recombinant wild-type and mutant thrombins (Table 2). With the exception of the mutant R67Q, all thrombins exhibited slow, tight binding inhibition (Figure 1). Values for K_i for both plasma (0.30 pM) and recombinant native thrombin (0.25 pM) were similar to previously published values (27, 30). The largest K_i value observed was for the mutant R67Q. Recombinant hirudin was a nonlinear competitive inhibitor of R67Q where the values 5.6 and 40.0 nM were obtained for K_{i1} and K_{i2} . These values were similar to the dysthrombin Quick I where K_{i1} and K_{i2} were 1.4 and 44.8 nM, respectively (31). Presumably, the mutant R67Q exists in two forms that have different affinities for hirudin as seen by thrombin Quick I. Arg⁶⁷ is partially buried in the ABE-I and forms part of an ion-pair cluster with residues Lys⁷⁰, Glu⁷⁷, and Glu⁸⁰ where it forms an ion-pair with Glu⁸⁰. The interactions are important for maintaining the integrity of the Lys⁷⁰-Glu⁸⁰ loop (35). Disruption of the ion-pair cluster by R67Q or R67C would distort this loop, thereby affecting several ionic and hydrophobic interactions critical for the formation of a tight inhibitor complex. The remaining thrombin K_i values varied from 0.53 pM for the mutant K110Q to 96.83 pM for R73Q.

Apart from the mutants R67Q and R73Q, the increase in K_i values were due mainly to a decrease in the k_{on} value. For the mutants R67Q and R73Q there is a major change in the value for k_{off} that contributes to the overall value of K_i .

Contribution of the ABE-I Residues to the Binding Energy. Small changes in binding energy ($\Delta\Delta G_b^{\circ}$) were observed with residues in the ABE-I not involved in ion-pair interactions with hirudin (Lys⁸¹, Lys¹⁰⁹, and Lys¹¹⁰). Substitution of these residues with glutamine resulted in a decrease of $\Delta\Delta G_b^{\circ}$ from 1.9 to 2.4 kJ mol⁻¹ (Table 3). Substitution of residues implicated in ionic interactions (Lys³⁶, Arg⁷³, Arg⁷⁵, and Arg^{77a}) resulted in greater decreases in $\Delta\Delta G_b^{\circ}$ except for Lys^{149e}, which is involved in an ion-pair with h-Asp⁵⁵ (Table 3). The greatest decrease was seen with R73Q (15.3 kJ mol⁻¹) with more modest decreases seen with the remaining mutants where the decrease varied from 3.6 kJ mol⁻¹ (R75Q) to 4.5 kJ mol⁻¹ (K36Q). A surprising result was seen with the mutant R35Q, which had a decrease in binding energy of 5.0 kJ mol⁻¹ since the only interaction made by this residue is between the NH1 of Arg³⁵ and the OE1 of h-Glu⁴⁹ through a mediating water molecule. The reciprocal mutation, h-E49Q has shown that this interaction is minimal (36). The residues of Lys^{60f}, Leu⁴⁰, Leu⁴¹, Phe^{60h}, and Glu³⁹ appear to form the $S_2' \rightarrow S_3'$ sites of thrombin. In the thrombin–hirudin complex the h-Glu⁴⁹ and h-His⁵¹ side chains occupy these sites and are involved in an intricate multicharge interaction involving the positive charges of Lys^{60f}, h-His⁵¹, and Arg³⁵ (via a mediating water molecule) and the negative charges of Glu³⁹, h-Glu⁴⁹, and possibly Glu¹⁹². It seems more likely that the R35Q substitution may have disrupted this network leading to a more severe effect than would be expected from the loss of an interaction with h-Glu⁴⁹.

Inhibition of Thrombin Mutants by rhir Mutants. Wild-type and mutant thrombins were used in kinetic studies against several rhir mutants to assess cooperative interactions in the interaction interface between the C-terminal tail of hirudin and ABE-I, using the double mutant cycle strategy. The kinetic parameters for the inhibition of native thrombin by the mutant hirudins h-D55N, h-E57Q, h-E58Q, h-E57–58Q, and h-E57–58–61–62Q were similar to that previously published by Betz and colleagues (24). The mutant hirudins h-D55N, E57Q, h-E57–58Q, and h-E57–58–61–62Q gave increases in K_i due mainly to decreases in k_{on} . Values for K_i for the inhibition of thrombin with h-E58Q differed with a large increase in k_{off} . The kinetic parameters for the inhibition of wild-type thrombin by h-E57–58Q were similar to those seen with h-E57Q. For h-E57–58Q, the double mutation of h-Glu⁵⁷ and h-Glu⁵⁸ only slightly increased the K_i value relative to the single substitutions. Interestingly, the large values for k_{off} observed for inhibition studies using h-E58Q was not apparent for h-E57–58Q. For h-E57–58–61–62Q, the effect of substituting residues h-Glu⁶¹ and h-Glu⁶² along with h-Glu⁵⁷ and h-Glu⁵⁸ has a significant effect on K_i (19.84 pM), where the rate of association ($3.8 \times 10^6 \text{ M}^{-1} \text{ s}^{-1}$) is severely affected and k_{off} only 2-fold greater than wild-type. Inhibition studies of the mutant thrombins tested against all the mutant hirudins showed a similar trend as with wild-type thrombin, however inhibition studies of R73Q with all the mutant hirudins and R77^aQ against h-D55N showed K_i values were affected by decreases in k_{on} and an increase in k_{off} .

Table 2: Kinetic Constants for the Interaction of Wild-Type and Mutant Thrombins with Mutants of Hirudin^a

form of IIa	form of hirudin																	
	rhir			h-D55N			h-E57Q			h-E58Q			h-E2Q ^c			h-E4Q ^c		
	$k_{\text{on}} \times 10^8$ (M ⁻¹ s ⁻¹)	$k_{\text{off}} \times 10^{-5}$ (s ⁻¹)	K_I (pM)	$k_{\text{on}} \times 10^8$ (M ⁻¹ s ⁻¹)	$k_{\text{off}} \times 10^{-5}$ (s ⁻¹)	K_I (pM)	$k_{\text{on}} \times 10^8$ (M ⁻¹ s ⁻¹)	$k_{\text{off}} \times 10^{-5}$ (s ⁻¹)	K_I (pM)	$k_{\text{on}} \times 10^8$ (M ⁻¹ s ⁻¹)	$k_{\text{off}} \times 10^{-5}$ (s ⁻¹)	K_I (pM)	$k_{\text{on}} \times 10^8$ (M ⁻¹ s ⁻¹)	$k_{\text{off}} \times 10^{-5}$ (s ⁻¹)	K_I (pM)	$k_{\text{on}} \times 10^8$ (M ⁻¹ s ⁻¹)	$k_{\text{off}} \times 10^{-5}$ (s ⁻¹)	K_I (pM)
pIIa	1.41	4.23	0.30	nd ^b	nd	nd	nd	nd	nd	nd	nd	nd	nd	nd	nd	nd	nd	nd
rIIa	1.24	3.10	0.25	0.53	3.29	0.62	0.24	5.45	2.27	1.16	21.81	1.88	0.24	7.00	2.92	0.038	7.54	19.84
R35Q	0.24	4.08	1.70	0.12	5.24	4.37	0.04	3.67	9.18	0.18	17.80	9.89	0.04	6.64	16.60	0.015	10.84	72.24
K36Q	0.29	4.18	1.44	0.10	2.64	2.64	0.04	3.68	9.20	0.20	18.82	9.41	0.04	6.83	17.08	0.013	8.22	63.26
R67Q ¹	0.0012	68.0	5616															
R67Q ²	nd	nd	40 065															
R73Q	0.02	19.37	96.83	0.02	18.69	93.45	0.005	20.70	413.94	0.01	35.65	356.52	0.005	24.96	499.14	0.0013	45.97	3536.5
R75Q	0.38	3.76	0.99	0.18	4.07	2.26	0.15	5.43	3.70	0.36	21.60	6.00	0.13	6.27	4.82	0.025	7.02	28.07
R77 ^a Q	0.36	4.72	1.61	0.34	22.13	6.51	0.09	3.74	4.15	0.33	22.94	6.95	0.15	6.81	4.54	0.035	7.72	22.07
K81Q	1.03	5.77	0.56	0.46	5.43	1.18	0.17	5.20	3.06	0.78	18.40	2.36	0.16	6.54	4.09	0.036	10.41	28.93
K109Q	0.71	4.40	0.62	0.31	5.55	1.79	0.11	4.47	4.31	0.67	24.59	3.67	0.13	6.99	5.38	0.032	10.87	33.96
K110Q	0.97	5.14	0.53	0.47	5.69	1.21	0.15	4.46	2.97	0.47	18.19	3.87	0.20	7.84	3.92	0.034	8.47	24.92
K149 ^c Q	0.79	4.52	0.58	0.86	10.32	1.20	0.08	2.24	2.80	0.41	14.59	3.56	0.17	8.18	4.81	0.031	9.77	31.52

^a Assays to determine the kinetic constants were performed and data analyzed as described in the Experimental Procedures. Standard errors for these assays were $\pm 10\%$ or less. ^b Not determined. ^c The mutants hirudins h-E57–58Q and h-E57–58–61–62Q are represented by h-E2Q and h-E4Q, respectively. Abbreviations: rhir is recombinant wild-type hirudin, pIIa and rIIa are wild-type plasma and recombinant thrombin, respectively.

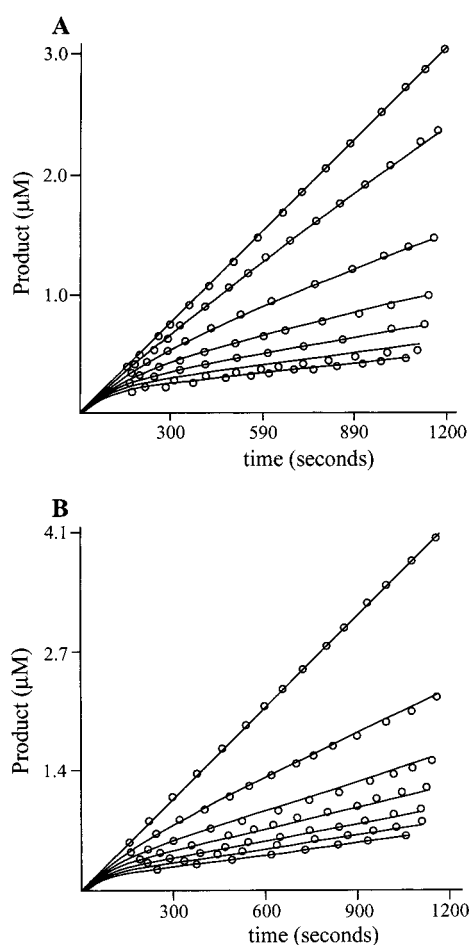


FIGURE 1: Slow tight binding inhibition of recombinant thrombin by hirudin. Panels A and B are representative of the progress curves obtained for the inhibition of native and mutant thrombins by recombinant native (rhir) and mutant hirudins. Panel A shows the progress curves obtained from the inhibition of wild-type thrombin (20 pM) with a range of rhir concentrations (10 pM \rightarrow 110 pM). Panel B shows the inhibition of the thrombin mutant R73Q (20 pM) with varying concentrations of rhir (2 nM \rightarrow 12 nM).

Coupling Energies for the Major Ion-Pair Interactions. The kinetic parameters for the inhibition of the ABE-I mutants of thrombin by recombinant hirudins h-D55N,

h-E57Q, and h-E58Q allowed the determination of cooperativity between basic residues in the thrombin ABE-I and acidic residues in the C-terminal tail of hirudin using the double mutant cycle strategy. In general, the values for $\Delta\Delta G_{\text{int}}^{\circ}$ were small for the majority of pairs of residues tested in double mutant cycles (Figure 2, Table 3) and reflected the absence of interactions between the residues in the thrombin–hirudin crystal structure. The major ion-pair interactions investigated in this study (Figure 3) were between h-Asp⁵⁵ with Arg⁷³ ($\Delta\Delta G_{\text{int}}^{\circ} = 2.4$ kJ mol⁻¹) and Lys^{149e} ($\Delta\Delta G_{\text{int}}^{\circ} = 0.6$ kJ mol⁻¹) and h-Glu⁵⁸ with Arg^{77a} ($\Delta\Delta G_{\text{int}}^{\circ} = 0.9$ kJ mol⁻¹). The low $\Delta\Delta G_{\text{int}}^{\circ}$ values for ion-pairs between Lys^{149e} and h-Asp⁵⁵ and h-Glu⁵⁸ with Arg^{77a} would suggest these interactions may not occur. In the thrombin–hirudin crystal structure an intermolecular ion pair is noted between h-Glu⁵⁷ and Arg⁷⁵ ($\Delta\Delta G_{\text{int}}^{\circ} = 2.3$ kJ mol⁻¹) but interestingly, a high coupling energy was seen for Arg^{77a} and h-Glu⁵⁷ ($\Delta\Delta G_{\text{int}}^{\circ} = 2.7$ kJ mol⁻¹). In general, the values for $\Delta\Delta G_{\text{int}}^{\circ}$ were raised for the interaction of h-Glu⁵⁷ with all mutant thrombins; however, due to the magnitude of $\Delta\Delta G_{\text{int}}^{\circ}$ for Arg⁷⁵ and Arg^{77a} with h-Glu⁵⁷, it is likely that h-Glu⁵⁷ forms direct interactions with both Arg^{77a} and Arg⁷⁵. High coupling energies were observed for some residues that are specially well separated. The coupling energies for the interaction of Arg⁷³ with h-Glu⁵⁷ ($\Delta\Delta G_{\text{int}}^{\circ} = 1.9$ kJ mol⁻¹) and h-Glu⁵⁸ ($\Delta\Delta G_{\text{int}}^{\circ} = 1.8$ kJ mol⁻¹) were raised and reflected an increase in k_{off} . The $\Delta\Delta G_{\text{int}}^{\circ}$ for Arg^{77a} against h-Asp⁵⁵ ($\Delta\Delta G_{\text{int}}^{\circ} = -1.7$ kJ mol⁻¹) indicated that substitution of these residues was especially disruptive.

DISCUSSION

Inhibition of thrombin by hirudin involves at least three steps for complex formation (37): an initial bimolecular step which involves the interaction between the thrombin ABE-I with the C-terminal tail of hirudin and a conformational change induced by the binding of the C-terminal tail within ABE-I which facilitates the occupation of the active site by the N-terminal domain of hirudin in the third step. This paper investigates the role of the thrombin ABE-I in “electrostatic steering” (25) and “ionic tethering” (26) in the initial stages of inhibitor complex formation.

Table 3: Free Energy and Coupling Energies for the Interaction of Mutant Thrombins with Mutant Hirudins^a

thrombin	hirudin										
	rhir		h-D55N			h-E57Q			h-E58Q		
	$-\Delta G_b^\circ$ (kJ mol ⁻¹)	$\Delta\Delta G_b^\circ$ (kJ mol ⁻¹)	$-\Delta G_b^\circ$ (kJ mol ⁻¹)	$\Delta\Delta G_b^\circ$ (kJ mol ⁻¹)	$\Delta\Delta G_{int}^\circ$ (kJ mol ⁻¹)	$-\Delta G_b^\circ$ (kJ mol ⁻¹)	$\Delta\Delta G_b^\circ$ (kJ mol ⁻¹)	$\Delta\Delta G_{int}^\circ$ (kJ mol ⁻¹)	$-\Delta G_b^\circ$ (kJ mol ⁻¹)	$\Delta\Delta G_b^\circ$ (kJ mol ⁻¹)	$\Delta\Delta G_{int}^\circ$ (kJ mol ⁻¹)
rIIa	74.8		72.4			69.1			69.6		
R35Q	69.8	5.0	67.4	5.0	0.0	65.5	3.6	1.4	65.3	4.2	0.7
K36Q	70.3	4.5	68.7	3.7	0.8	65.5	3.6	0.9	65.4	4.2	0.3
R73Q	59.5	15.3	59.5	12.9	2.4	55.7	13.4	1.9	56.1	13.5	1.8
R75Q	71.2	3.6	69.1	3.3	0.3	67.8	1.3	2.3	66.6	3.0	0.6
R77 ^a Q	70.5	4.3	66.4	6.0	-1.7	67.5	1.6	2.7	66.2	3.4	0.9
K81Q	72.7	2.1	70.8	1.6	0.5	68.3	0.8	1.3	69.0	0.6	1.5
K109Q	72.4	2.4	69.7	2.7	-0.3	67.5	1.6	0.8	67.9	1.7	0.7
K110Q	72.9	1.9	70.8	1.6	0.3	68.4	0.7	1.2	67.7	1.9	0.0
K149 ^e Q	72.6	2.2	70.8	1.6	0.6	68.6	1.7	1.7	67.9	1.7	0.5

^a Values for ΔG_b° and $\Delta\Delta G_b^\circ$ were determined from the kinetic data presented in Table 2 as described in the Experimental Procedures. Abbreviations: rhir is recombinant wild-type hirudin and rIIa refers to recombinant wild-type thrombin.

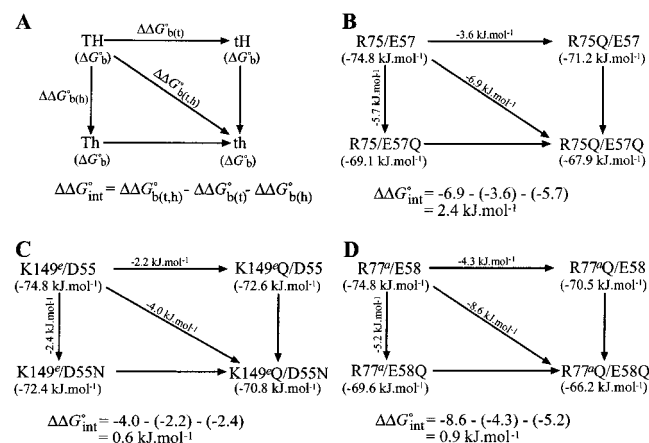


FIGURE 2: Determining the coupling energy using the double mutant cycle strategy. Double mutant cycles were constructed as shown in the Experimental Procedures and panel A. Panels B, C, and D are representative for double mutant cycles constructed and the coupling energy determined for the mutant thrombins and hirudins.

ABE-I Basic Residues Contribute to the Positive Electrostatic Field Necessary for Electrostatic Steering. Asymmetric complementary electrostatic fields generated by the thrombin ABE-I and the C-terminal tail of hirudin which are important for their preorientation and rate enhancement for complex formation by electrostatic steering (25). The C-terminal tail of hirudin has a cluster of several negatively charged residues, two of these residues, h-Glu⁶¹ and h-Glu⁶² do not make direct interactions with the thrombin ABE-I but contribute between 1 and 2 kJ/mol⁻¹ to the binding energy (24, 25). Likewise, substitution of ABE-I residues Lys⁸¹, Lys¹⁰⁹, and Lys¹¹⁰ with glutamine gave corresponding decreases in the binding energy which reflected a decrease in the association rate constant. A similar decrease in ΔG_b° was also seen for the K14 substitution. A higher ΔG_b° value was expected for this interaction as Lys^{149e} makes a ion-pair with the h-Asp⁵⁵ according to the thrombin–hirudin crystal structure (17). A double mutant cycle was constructed and the derived coupling energy (Figure 2) suggests this interaction is unlikely to occur in solution (see below). The two residues Arg³⁵ and Arg⁶⁷ make no major contacts with hirudin in the thrombin–hirudin crystal structure, however, when substituted give greater decreases in ΔG_b° than expected. Both substitutions appear to have an effect on

complex formation by affecting local protein structure rather than the loss of a contact. Therefore, the residues Arg³⁵, Arg⁶⁷, Lys⁸¹, Lys¹⁰⁹, Lys¹¹⁰, and Lys^{149e} appear to contribute mainly to the positive electrostatic field generated by the thrombin ABE-I and is necessary for productive complex formation by interacting with the complementary and asymmetric negative electrostatic field generated by the hirudin C-terminal tail by electrostatic steering.

Contribution to the Binding Energy by the Thrombin ABE-I Residues Involved in “Ionic Tethering”. Direct ionic interactions between ABE-I and hirudin are also important in complex formation. The formation of ion pairs, termed “ionic tethering” (26), may be important in tethering the C-terminal tail in ABE-I allowing short-range hydrophobic interactions to occur leading to a hydrophobic core between the hirudin and ABE-I interaction interface (38–40). The thrombin–hirudin crystal structure (17) shows several ion-pair interactions between ABE-I and hirudin residues that could be involved in ionic tethering (Figure 3). Arg⁷³ forms a good hydrogen bonded ion-pair with h-Asp⁵⁵. The residue Arg⁷⁵ forms an ion-pair with h-Glu⁵⁷ from a neighboring molecule in the crystal lattice. Arg^{77a} forms an ion-pair with h-Glu⁵⁸ and a water mediated solvent interaction with h-Glu⁵⁷, while Lys³⁶ forms an ion-pair with the carboxylate of h-Gln⁶⁵ (3.3 Å). The residues Lys³⁶, Arg⁷³, Arg⁷⁵, and Arg^{77a} all contributed higher free energies when substituted with glutamine; a result consistent with their observed interactions in the thrombin–hirudin structure (17), but were slightly smaller than expected, presumably due to solvent effects. Indeed, these data are consistent with theoretical calculations made by Karshikov et al. (25), for the loss of binding energy for the removal of complementary charges in hirudin using the modified Tanford–Kirk procedure and by Sharp (41) who used a modified finite-difference Poisson–Boltzman (FDPB) method. Reciprocal mutations in hirudin gave, in general, similar changes in binding energy; however, the h-D55N substitution gave an unexpected small change in binding energy (2.3 kJ/mol⁻¹) than what would be expected for the loss of an ion-pair interaction. However, it seems plausible that the asparagine side chain may make new and additional contacts that compensate for the loss of the ion-pair. The crystal structure of the 456EGF domains of thrombomodulin complexed with thrombin (42) shows a major hydrophobic association of the thrombomodulin Tyr⁴¹³–Ile⁴¹⁴–Leu⁴¹⁵

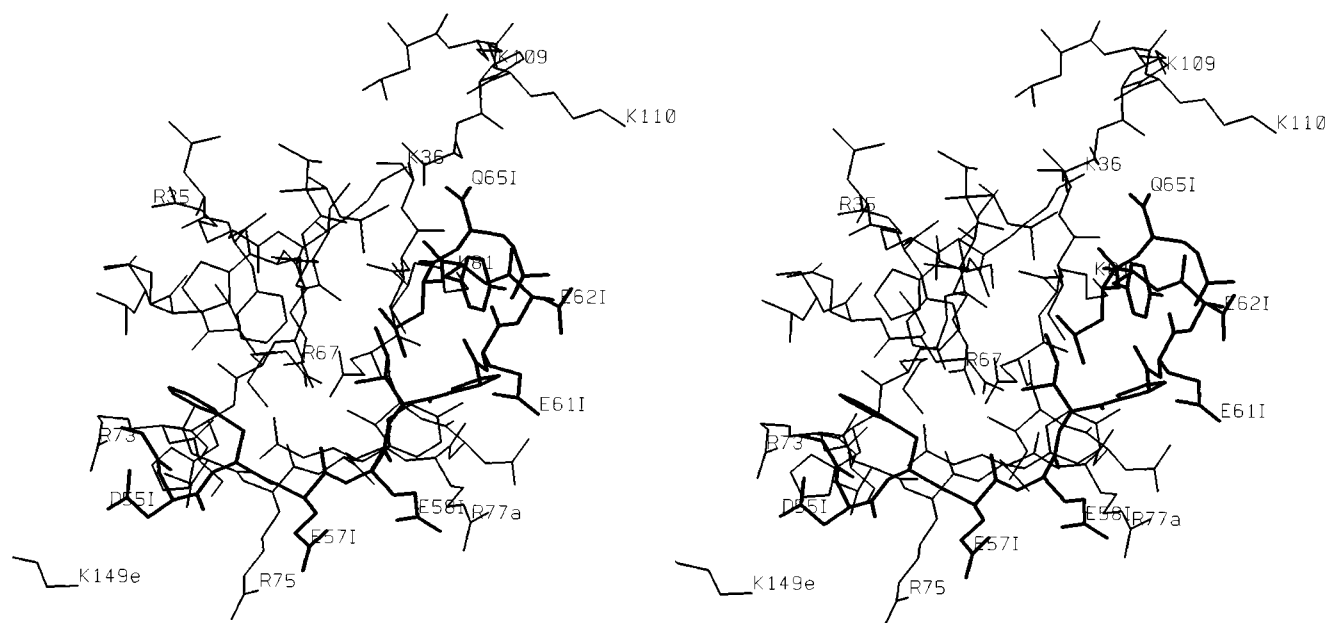


FIGURE 3: Stereodiagram for the binding of the C-terminal tail of hirudin in the thrombin ABE-I. The figure was drawn using RasMol v2.5 using the pdb file 4HTC. The hirudin residues 55–65 (bold lines) are shown in complex with thrombin ABE-I (thin lines). Hirudin residues are numbered with the suffix “I”.

triplet bound in a hydrophobic depression formed by residues Phe³⁴, Leu⁴⁰, Thr⁷⁴, Tyr⁷⁶, and Ile⁸² where there were no major interactions with Arg⁷³. Hence, hydrophobic interactions could substitute for ionic interactions with Arg⁷³. Furthermore, the double mutation of R77^aQ and h-D55N is especially unstable for complex formation ($\Delta\Delta G_{\text{int}}^{\circ} = -1.7$, see below; $k_{\text{off}} = 22.13 \times 10^5 \text{ s}^{-1}$), suggesting that the Arg^{77a} substitution destabilizes the compensating interactions made by h-D55N.

The majority of the ABE-I basic residues involved in ionic tethering contribute to the association rate constant but not to the stabilization of the complex. Previous studies by Stone and Hofsteenge (27) show that electrostatic interactions contribute predominantly to the association rate constant while hydrophobic interactions stabilize the inhibitor complex (38–40). Ionic tethering therefore appears to enhance the rate at which the highly flexible C-terminal tail adopts an appropriate conformation within ABE-I allowing numerous short-range hydrophobic interactions to occur. Several hydrophobic residues are involved in the stabilization of the C-terminal tail in ABE-I. The phenyl ring of h-Phe⁵⁶ is buried in a hydrophobic pocket formed by residues Phe³⁴, Leu⁴⁰, Arg⁷³, and Thr⁷⁴. The remaining hirudin C-terminal hydrophobic residues are located on one side of a 3_{10} helical turn which form a hydrophobic core with thrombin residues Leu⁶⁵, Tyr⁷⁶, and Ile⁸² (Figure 3).

Probing the Thrombin–Hirudin Interaction Interface Using Double Mutant Cycles. The coupling energy ($\Delta\Delta G_{\text{int}}^{\circ}$) was calculated for the major ion-pair interactions between basic residues in ABE-I and acidic residues in the C-terminal tail of hirudin. The hirudin residue h-Asp⁵⁵ makes two ion-pair interactions with thrombin residues Lys^{149e} and Arg⁷³. Calculation of the coupling energies suggests that the interaction between Lys^{149e} and h-Asp⁵⁵ is unlikely to exist. A moderate coupling energy was seen for the ion-pair interaction between Arg⁷³ and h-Asp⁵⁵, however, it was also raised for h-Glu⁵⁷ and h-Glu⁵⁸, both of which make no direct

contacts with Arg⁷³. In both cases, the raised coupling energy is paralleled by large losses in binding energy with corresponding increases in k_{off} indicating that substitution of Arg⁷³ leads to destabilization of the hirudin tail in the ABE-I. Two possibilities are likely to occur. First, the h-Asp⁵⁵/Arg⁷³ ion-pair may play critical role in tethering the C-terminal tail in ABE-I facilitating h-Glu⁵⁷ and h-Glu⁵⁸ to form respective ion-pairs in ionic tethering. Second, the R73Q substitution could induce a conformational change which would affect several interactions at the thrombin–hirudin interface. Evidence against a major conformational change induced by the R73Q substitution is normal catalysis toward chromogenic substrates and mild changes in activity against fibrinogen and thrombomodulin (5) compared to the severe effect on inhibition of by hirudin and HCII (8). Arg⁷³ is at the pass formed by the Phe³⁴-Leu⁴¹ and Lys⁷⁰-Glu⁸⁰ loops of thrombin where the C-terminal tail interacts through this pass by binding to the S' subsites on the N-terminal side and the ABE-I on the C-terminal side. Therefore, it is plausible that the h-Asp⁵⁵/Arg⁷³ ion-pair is important in tethering the C-terminal tail in ABE-I allowing interactions to occur within the S' subsites and ionic tethering between ABE-I and the hirudin C-terminal tail.

The crystal structure of hirudin with thrombin shows an ion-pair interaction between Arg⁷⁵ of thrombin and a symmetry related contact with h-Glu⁵⁷ in a neighboring complex in the crystal lattice. There is also a water mediated solvent bridge between h-Glu⁵⁷ and Arg^{77a} and a major ion-pair interaction between Arg^{77a} and h-Glu⁵⁸. Inhibition studies of the ABE-I mutants with h-E57Q showed elevated $\Delta\Delta G_{\text{int}}^{\circ}$ values for most of the ABE-I mutants tested, indicating some degree of cooperativity between h-Glu⁵⁷ and the ABE-I residues. This could be due to a minor perturbation in the structure due to the mutation. The h-Glu⁵⁷ residue forms a number of hydrogen bonds, the amide nitrogen with Thr⁷⁴, the OE2 forms another with Tyr⁷⁶ and finally the carbonyl oxygen makes a water mediated hydrogen bond with the

guanidium group of Arg⁶⁷. Disruption of any of these bonds could lead to a structural perturbation affecting the stability of the thrombin–hirudin complex. However, two high coupling energies were seen for mutant cycles constructed for thrombins Arg⁷⁵, Arg^{77a}, and h-Glu⁵⁷. The high $\Delta\Delta G_{\text{int}}^{\circ}$ value for Arg⁷⁵ suggests that a direct interaction may exist between Arg⁷⁵ and h-Glu⁵⁷ in solution as opposed to the ion-pair between Arg⁷⁵ and h-Glu⁵⁷ in a neighboring molecule seen in the crystal structure. This indicates the intermolecular ion-pair seen in the crystal structure is due to crystal packing conditions (17). The same structure shows Arg^{77a} forming a solvent bridge with h-Glu⁵⁷; this contact is supported by the $\Delta\Delta G_{\text{int}}^{\circ}$ value of 2.7 kJ mol⁻¹.

The thrombin–hirudin crystal shows a ion-pair between Arg^{77a} and h-Glu⁵⁸ although the electron density of C β and C γ of the h-Glu⁵⁸ is poor and disordered. The low value for the coupling energy (0.9 kJ mol⁻¹) for these residues in double mutant cycles indicates that this interaction is weak. The crystal structures of thrombin–hirugen (43) and thrombin–hirulog-3 (44) also have equally disordered electron density for the h-Glu⁵⁸ side chain, suggesting protection against β -cleavage at Arg^{77a} by bound hirugen or hirulog-3 may be due more to a physical hindrance than a direct interaction between Arg^{77a} and h-Glu⁵⁸ (44). Since there is large increase in K_{I} for the inhibition of thrombin with the h-E58Q substitution, it is therefore interesting to speculate as to why there is such a large effect assuming this residue makes a minor interaction with Arg^{77a}. Studies by Betz and colleagues (24) have shown that h-Glu⁵⁷ and h-Glu⁵⁸ act cooperatively. The increase in K_{I} associated with the substitution of h-Glu⁵⁸ side chain may be due to the amide nitrogen of glutamine interacting directly with the carboxylate of the h-Glu⁵⁷ side chain. Such an interaction would undoubtedly have distorted the interaction between Arg^{77a} and h-Glu⁵⁷ in the complex giving rise to the loss of binding energy. Inhibition of the wild-type and ABE-I mutant thrombins by h-E58Q are associated with a large increase in k_{off} , but by comparison, mutation of h-Glu⁵⁷ to glutamine does not greatly increase the value of k_{off} when tested against the thrombin mutants. However, for the interaction of mutant thrombin residues R75Q and R77^Q with h-E57–58Q and h-E57–58–61–62Q their is an increase in K_{I} due mainly to a decrease of k_{on} . The elevated k_{off} associated with h-E58Q was not observed for the interactions involving the double mutant. This indicates that once the h-Glu⁵⁷ residue is substituted by a glutamine, the h-E58Q side chain no longer makes a direct contact with the h-E57Q side chain. This may relieve the structural perturbation caused by the contact formed between the h-E58Q and h-Glu⁵⁷ side chains allowing the C-terminal tail of hirudin to adopt a conformation within ABE-I leading to stable complex formation.

In conclusion, the initial events in complex formation between thrombin and hirudin involve first; the interaction between complementary and asymmetric electric fields that preorientate and increase the rate of complex formation between the two molecules by electrostatic steering (24). Once the complex is held loosely together by general electrostatic forces, we propose direct interactions are made by Arg⁷³ with h-Asp⁵⁵, Arg⁷⁵ and Arg^{77a} with h-Glu⁵⁷, and Lys³⁶ with h-Gln⁶⁵ ensure correct positioning of C-terminal tail of hirudin within ABE-I by “ionic tethering” (26). Tethering the C-terminal tail of hirudin in ABE-I would allow

short-range hydrophobic interaction to occur leading to a hydrophobic core in the interaction interface between thrombin and hirudin (38–40), which in turn leads to the final tight binding step by occlusion of the active site by the N-terminal domain of hirudin. It is likely that the formation of complexes between thrombin and all its ligands mediated through ABE-I utilize a similar strategy, where complementary electrostatic fields enhance the rate of complex formation by electrostatic steering, and that ionic tethering ensures the complex is stabilized.

ACKNOWLEDGMENT

We would like to thank Prof. Arthur Lesk, Dept of Hematology, University of Cambridge, Cambridge, U.K., and Dr. Paul Hopkins, Gladstone Institute, San Francisco, for the critical reading of this manuscript.

REFERENCES

- Stubbs, M. T., and Bode, W. (1993) *Thromb. Res.* 69, 1–58.
- Hofsteenge, J., and Stone, S. R. (1987) *Eur. J. Biochem.* 168, 49–56.
- Hofsteenge, J., Braun, P. J., and Stone, S. R. (1988) *Biochemistry* 27, 2144–2151.
- Binnie, C. G., and Lord, S. T., (1993) *Blood* 81, 3186–3192.
- Tsiang M., Jain A. K., Dunn K. E., Rojas, M. E., Leung, L. L. K., and Gibbs, C. S. (1995) *J. Biol. Chem.* 270, 16854–16863.
- Berliner, L. J., Sugawara, Y., and Fenton J. W. (1985) *Biochemistry* 24, 7005–7009.
- Sheehan, J. P. Wu, Q., Tollefsen, D. M., and Sadler, J. E. (1993) *J. Biol. Chem.* 268, 3639–3645.
- Myles, T., Church F. C., Whinna H. W., Monard D., and Stone S. R. (1998) *J. Biol. Chem.* 273, 31203.
- Liu, L. W., Vu, T. K. H., Esmon C. T., and Coughlin, S. R. (1991) *J. Biol. Chem.* 266, 16977–16980.
- Mathews, I. I., Padmanabhan, K. P., Ganesh, V., Tulinsky, A., Ishii, M., Chen, J., Turk C. W., Coughlin, S., and Fenton, J. W. (1994) *Biochemistry* 33, 3266–3279.
- Hofsteenge, J., Taguchi, H., and Stone, S. R. (1986) *Biochem. J.* 237, 243–251.
- Hofsteenge, J., and Stone, S. R., (1987) *Eur. J. Biochem.* 168, 49–56.
- Henriksen, R. A., and Mann, K. G. (1988) *Biochemistry* 27, 9160–9165.
- Stone, S. R., Braun, P. J., and Hofsteenge, J. (1987) *Biochemistry* 26, 4617–4624.
- Grütter, M., Priestle, J. P., Rahuel, J., Grossenbacher, H., Bode, W., Hofsteenge, J., and Stone, S. R. (1990) *EMBO J.* 9, 2361–2365.
- Rydel, T. J., Ravichandran, K. G., Tulinsky, A., Bode, W., Huber, R., Roitsch, C., and Fenton, J. W. (1990) *Science* 249, 277–280.
- Rydel, T. J., Tulinsky, A., Bode, W., and Huber, R. (1991) *J. Mol. Biol.* 221, 583–601.
- Sheehan, J. P., and Sadler, J. E. (1994) *Proc. Natl. Acad. Sci. U.S.A.* 91, 5518–5522.
- Gan, Z. R., Li, Y., Chen, Z., Lewis, S. D., and Shafer, J. A. (1994) *J. Biol. Chem.* 269, 1301–1305.
- Wallace A., Rovelli, G., Hofsteenge, J., and Stone, S. R. (1989) *Biochem. J.* 257, 1919–1926.
- Stone, S. R., Brown-Luedi, M. L. Rovelli, G., Guidolin, A., McGlynn, E., and Monard, D. (1994) *Biochemistry* 33, 7731–7735.
- Esmon, C. T., and Lollar, P. (1996) *J. Biol. Chem.* 271, 13882–13887.
- Stone, S. R., Dennis, S., and Hofsteenge, J. (1989) *Biochemistry* 28, 6857–6863.
- Betz, A., Hofsteenge, J., and Stone, S. R. (1991) *Biochem. J.* 275, 801–803.

25. Karshikov, A., Bode, W., Tulinsky, A., and Stone, S. R. (1992) *Protein Sci.* 1, 727–735.
26. Wade, R. C., Gabdoulline, R. R., Lüdemann, S. K., and Lounnas, V. (1998) *Proc. Natl. Acad. Sci. U.S.A.* 95, 5942–5949.
27. Stone, S. R., and Hofsteenge, J. (1986) *Biochemistry* 25, 4622–4628.
28. Chase, T., and Shaw, E. (1969) *Biochemistry* 8, 2212–2224.
29. Braun, P. J., Dennis, S., Hofsteenge, J., and Stone, S. R. (1988) *Biochemistry* 27, 6517–6522.
30. Morrison, J. F. (1982) *Trends Biochem. Sci. (March)*, 102–105.
31. Stone, S. R., Schmitz, T., Henriksen, S. A., Hofsteenge, J., and Dodt, J. (1991) *Biochemistry* 30, 6392–6397.
32. Wells, J. A. (1990) *Biochemistry* 29, 8509–8517.
33. Horovitz, A., and Fersht, A. R. (1990) *J. Mol. Biol.* 214, 613–617.
34. Myles, T., Le Bonniec, B. F., and Stone, S. R. (1993) *Thromb. Haemostas.* 69, 1239.
35. Bode, W., Turk, D., and Karshikov, A. (1992) *Protein Sci.* 1, 426–471.
36. Betz, A., Hopkins, P. C. R., Le Bonniec, B. F., and Stone, S. R. (1994) *Biochem. J.* 298, 507–510.
37. Jackman, M. P., Parry, M. A. A., Hofsteenge, J., and Stone, S. R. (1992) *J. Biol. Chem.* 267, 15357–15383.
38. Tsuda, Y., Szewczuk, Z., Wang, J., Yue, S. Y., Purisima, E., and Konishi, Y. (1995) *Biochemistry* 34, 8708–8714.
39. Wang, J., Szewczuk, Z., Yue, S. Y., Tsuda, Y., Konishi, Y., and Purisima, E. O. (1995) *J. Mol. Biol.* 253, 473–492.
40. Cheng, Y., Slon-Usakiewisc, J. J., Wang, J., Purisima, E. O., and Konishi, Y. (1996) *Biochemistry* 35, 13021–13029.
41. Sharp, K. (1996) *Biophys. Chem.* 61, 37–49.
42. Fuentes-Prior, P., Iwanaga, Y., Huber, R., Pagila, R., Rumennik, G., Seto, M., Morser, J., Light, D. R., and Bode, W. (2000) *Nature* 404, 518–525.
43. Skrzypczak-Jankun, E., Carperos, V., Ravichandran, K. G., Tulinsky, A., Westbrook, M., and Maraganore, J. M. (1991) *J. Mol. Biol.* 221, 1379–1393.
44. Qui, X., Padmanabhan, K., Carperos, V. E., Tulinsky, A., Kline, T., Maraganore, J. M., and Fenton, J. W. (1992) *Biochemistry* 31, 11689–11697.
45. van der Locht, A., Lamba, D., Baur, M., Huber, R., Friedrich, T., Kröger, B., Höffken, W., and Bode, W. (1995) *EMBO J.* 14, 5149–5157.

BI0023549